2014 IEEE International Conference on Robotics & Automation (ICRA)
Hong Kong Convention and Exhibition Center
May 31 - June 7, 2014. Hong Kong, China

Nonparametric Cooperative Tracking in Mobile Ad-Hoc Networks

Mao Shan, *Member, IEEE,* Stewart Worrall, *Member, IEEE,* Eduardo Nebot, *Senior Member, IEEE*
Australian Centre for Field Robotics
The University of Sydney, NSW 2006, Australia
{m.shan, s.worrall, nebot}@acfr.usyd.edu.au

***Abstract*— This paper presents a new nonparametric approach for cooperative localisation and tracking by fusing relative range measurements between mobile network equipped nodes. Standard approaches based on parametric methods are known to be limited to problems that contain Gaussian properties. This paper overcomes this limitation by proposing a novel particle filter based cooperative tracking approach that is suitable for mobile ad-hoc networks (MANETs). The filter maintains the marginal state of every node instead of a joint state of the group, and updates the estimates using a Gibbs sampler, which is known as a Markov chain Monte Carlo (MCMC) method. The performance of the proposed algorithm is demonstrated by examining 16 mobile nodes moving randomly while sharing information with neighbouring nodes in a MANET. The results show that the proposed approach facilitates the tracking of mobile nodes that do not have egocentric position information available. It also outperforms the EKF in systems with non-Gaussian properties.**

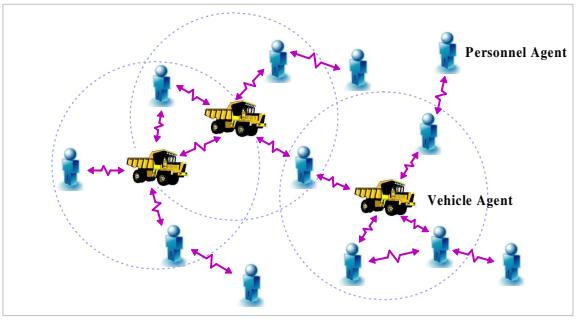

Fig. 1. Cooperative tracking in a mobile ad-hoc network. The figure demonstrates a typical cooperative tracking application where every mobile node (vehicle or personnel agent) is connected with others nearby to form a mesh network.

I. Introduction

Localising and tracking mobile nodes in an industrial environment is necessary for many autonomous and manned system applications. Different forms of GPS-based tracking algorithms are widely used for this purpose. Unfortunately, in some environments, GPS-based systems have difficulties in maintaining an accurate position due to problems such as GPS satellite availability, signal multipath, etc. An alternate approach is to use a number of beacons located at known positions to estimate the agent location, and the mobile agent is fitted with a range/bearing sensor capable of detecting and identifying the beacons. Trilateration/triangulation algorithms, often involving filters such as Kalman filter, are used to estimate the position. This technique requires the working environment to be covered by a sufficient number of beacons to ensure that good position accuracy can be achieved.

The tracking problem can also be addressed by using cooperative localisation/tracking. Measurements of relative range/bearing can be obtained using time of arrival (TOA) [1], angle of arrival (AOA) [2], phase measurements, received signal strength (RSS) [3], and so on. They are used to estimate the relative positions of all mobile nodes. This type of approach can have significant advantages, since it can reduce or eliminate the requirement for fixed beacons, and the requirement for absolute position information (i.e., GPS) from all of the mobile nodes.

A typical cooperative tracking example can be seen in Figure 1. In this case the mobile nodes are moving in a given area of operation, and the absolute Euclidean positions and pairwise measurements are shared between the nodes via a type of peer-to-peer (P2P) communication such as a wireless sensor network (WSN) [3] [4], mobile ad-hoc network (MANET) [5] or vehicular ad-hoc network (VANET) [6]. The information can then be used to update the position estimates of each mobile node at a central point, such as a base station.

This paper presents a novel cooperative tracking algorithm that makes use of a MANET. This method requires a mesh network for P2P communication and the distances between nearby mobile nodes. A Gibbs sampler based cooperative particle filter (GSCPF), particularly for nonparametric cooperative tracking, is proposed to estimate the state of every mobile node. This filter incorporates all available egocentric and relative inter-node observations, and can be implemented in a centralised or decentralised architecture. The proposed algorithm has the importance sampling step in a classical particle filter replaced by a Gibbs sampler, which is a Markov chain Monte Carlo (MCMC) method. The Gibbs sampler is able to sample from each low-dimensional target space conditionally on others, rather than directly from the high-dimensional joint state. The main contribution of paper is to provide a more generalised approach for cooperative tracking for cases where the Gaussian assumption is not valid.

The remainder of the paper is organised as follows. Section II reviews the related work in the area of cooperative localisation/tracking. Section III formulates the problem in the Bayesian form. A detailed description of the proposed tracking algorithm is presented in Section IV and testing results in Section V. Finally, conclusions and future work are presented in Section VI.

978-1-4799-3684-7/14/$31.00 ©2014 IEEE

II. Related Work

The advent of efficient P2P communication technology has made the cooperative localisation (CL) an active area of research. An comprehensive review of current work is presented in [1]. Current CL approaches can be categorised into parametric and nonparametric methods. The parametric include Kalman filter (KF) and extended Kalman filter (EKF) based [5] [7] [8] [9], maximum likelihood estimation (MLE) based [10], maximum *a posteriori* (MAP) based [11], least-squares (LS) based [12] [13] methods to name a few. The nonparametric approaches are mostly particle filter (PF) based [4] [14] [15] [16], such as nonparametric belief propagation (NBP), sum-product algorithm over a wireless network (SPAWN) and so forth. Among them, the EKF is often the most attractive due to the minimal computational cost. Nevertheless, the application of these parametric approaches is limited to problems presenting Gaussian properties.

PF based algorithms are considered the ideal choice for tracking of multiple objects in cluttered scenarios in which the Gaussian assumption is not valid. The most intuitive way to track every node cooperatively is to maintain a joint state. However, the "dimensional curse" brought by a high-dimensional state space remains a challenge, particularly when parametric filtering methods are not applicable. Generally speaking, ensemble size required in PF grows exponentially with the number of nodes [17]. By marginalising some variables, a Rao-Blackwellised particle filter (RBPF) [18] can outperform a standard PF with a reduced state space size. The prerequisite is that a subset of the state space can be handled by a parametric filtering approach.

The NBP was initially proposed for localising in static networks [19]. Its variants can be used for cooperative tracking in mobile networks [20]. Generally, it is a distributed message-passing method on a graphical model. However, it is only guaranteed to converge to the correct beliefs in singly connected networks (e.g., tree). Overconfident results would be obtained for networks multiply connected, or in other words networks with loops/cycles in terms of factor graphs [21] [22]. The same limitation is also found in the SPAWN [1]. Only few solutions for networks with loops exist in the literature and they are rarely used in localisation [23].

III. Bayesian Formulation on Cooperative Tracking

Suppose a joint state representing a set of N_n nodes moving in a field:

$$\mathbf{X} = \left[\left(\mathbf{x}^1\right)^T \quad \left(\mathbf{x}^2\right)^T \quad \cdots \quad \left(\mathbf{x}^{N_n}\right)^T \right]^T$$

To track the joint state cooperatively, a filter propagates it from time $k-1$ to k and updates estimates with all observations at time k.

$$P\left(\mathbf{X}_k|\mathbf{Z}_{1:k}\right) \propto P\left(\mathbf{Z}_k|\mathbf{X}_k\right) \times \int P\left(\mathbf{X}_k|\mathbf{X}_{k-1}\right) P\left(\mathbf{X}_{k-1}|\mathbf{Z}_{1:k-1}\right) d\mathbf{X}_{k-1} \tag{1}$$

We make the following assumptions:

- every node moves independently in the field, from which we have: $P\left(\mathbf{X}_k|\mathbf{X}_{k-1}\right) = \prod_{p=1}^{N_n} P\left(\mathbf{x}_k^p|\mathbf{x}_{k-1}^p\right)$.
- an egocentric position observation $\mathbf{z}_k^p$ regarding node p is only dependent on the current state of the node $\mathbf{x}_k^p$.
- a relative range observation $\mathbf{z}_k^{p\to q}$ $(p \neq q)$ is only conditional on the current state of two involved nodes.

Therefore, the observation component in Equation (1) is able to be factorised to egocentric and relative observations.

$$P\left(\mathbf{Z}_k|\mathbf{X}_k\right) = \left(\prod_{p=1}^{N_n} P\left(\mathbf{z}_k^p|\mathbf{x}_k^p\right)\right)\left(\prod_{p=1}^{N_n}\prod_{q=1}^{N_n} P\left(\mathbf{z}_k^{p\to q}|\mathbf{x}_k^p,\mathbf{x}_k^q\right)\right)$$

where $p \neq q$.

A marginal distribution $P\left(\mathbf{x}_k^p|\mathbf{Z}_{1:k}\right)$ for node p at time k could be obtained by integrating the joint posterior in Equation (1) with respect to the joint state of the rest nodes (denoted by $\bar{\mathbf{X}}_k$). This is achieved by:

$$P\left(\mathbf{x}_k^p|\mathbf{Z}_{1:k}\right) = \int P\left(\mathbf{X}_k|\mathbf{Z}_{1:k}\right) d\bar{\mathbf{X}}_k \tag{2}$$

where $\mathbf{X}_k = \left[\left(\mathbf{x}_k^p\right)^T \quad \bar{\mathbf{X}}_k^T \right]^T$

IV. A Particle Filter for Cooperative Tracking

A. Theory

The proposed algorithm keeps the marginal state of each node, which is tracked independently. Suppose at time k, each of N_n mobile nodes is tracked by a discrete set of L particles, we have:

$$\Theta_k = \begin{bmatrix} \{\mathbf{x}_k^{1,(i)}, w_k^{1,(i)}\}_{i=1}^L \sim P\left(\mathbf{x}_k^1|\mathbf{Z}_{1:k}\right) \\ \vdots \\ \{\mathbf{x}_k^{N_n,(i)}, w_k^{N_n,(i)}\}_{i=1}^L \sim P\left(\mathbf{x}_k^{N_n}|\mathbf{Z}_{1:k}\right) \end{bmatrix}$$

For each time step and each target node p, we infer a joint posterior with an incomplete observation set:

$$\begin{aligned} P_{\mathbf{X}_k} &\triangleq P\left(\bar{\mathbf{X}}_k|\mathbf{x}_k^p,\mathbf{Z}_k\right) P\left(\mathbf{x}_k^p|\mathbf{Z}_{1:k}\right) \\ &= \frac{P\left(\bar{\mathbf{X}}_k,\mathbf{x}_k^p|\mathbf{Z}_k\right)}{P\left(\mathbf{x}_k^p|\mathbf{Z}_k\right)} \times \frac{P\left(\mathbf{Z}_k|\mathbf{x}_k^p\right) P\left(\mathbf{x}_k^p|\mathbf{Z}_{1:k-1}\right)}{P\left(\mathbf{Z}_k|\mathbf{Z}_{1:k-1}\right)} \\ &\propto P\left(\mathbf{Z}_k|\mathbf{X}_k\right) \int P\left(\mathbf{x}_k^p|\mathbf{x}_{k-1}^p\right) P\left(\mathbf{x}_{k-1}^p|\mathbf{Z}_{1:k-1}\right) d\mathbf{x}_{k-1}^p \end{aligned} \tag{3}$$

Please note that the joint posterior $P_{\mathbf{X}_k}$ does not contain prior knowledge of nodes except for node p. These nodes grouped in $\bar{\mathbf{X}}_k$ are defined as "auxiliary nodes", for they are temporarily aggregated together to help track the "primary node" p. The auxiliary nodes are then marginalised away:

$$P\left(\mathbf{x}_k^p|\mathbf{Z}_{1:k}\right) = \int P\left(\bar{\mathbf{X}}_k|\mathbf{x}_k^p,\mathbf{Z}_k\right) P\left(\mathbf{x}_k^p|\mathbf{Z}_{1:k}\right) d\bar{\mathbf{X}}_k \tag{4}$$

The resultant marginal distribution $P\left(\mathbf{x}_k^p|\mathbf{Z}_{1:k}\right)$ of the primary node state $\mathbf{x}_k^p$ is inferred with a full set of observations up to time k. It is identical to that in Equation (2).

B. Gibbs Sampling

The joint posterior distribution $P_{\mathbf{X}_k}$ in Equation (3) is usually too complicated to sample from directly. Instead, a Gibbs sampler is introduced to sample from conditional distributions.

Define N_n variables $\theta^1, \cdots, \theta^{N_n}$ corresponding to all N_n nodes in $P_{\mathbf{X}_k}$. A replacing joint distribution is written as:

$$\begin{aligned} &P\left(\theta^1, \cdots, \theta^{p-1}, \theta^p, \theta^{p+1}, \cdots, \theta^{N_n}\right) \\ &= P\left(\bar{\mathbf{X}}_k | \mathbf{x}_k^p, \mathbf{Z}_k\right) P\left(\mathbf{x}_k^p | \mathbf{Z}_{1:k}\right) \end{aligned}$$

Initialise these variables deterministically or randomly:

$$\theta^1 = \theta_0^1, \cdots, \theta^{N_n} = \theta_0^{N_n}$$

The sampler draws a sample from the conditional distribution of each variable given the remaining variables at a time. A traversal of all N_n variables is defined as a scan of the sampling. When nodes are assumed to be mutually independent at the first iteration, *a priori* information of the nodes could be safely incorporated into the filtering. To achieve this, for each node q at each scan $j \geq 1$, we sample:

$$\begin{aligned} \theta_j^q &\sim P\left(\theta^q | \theta_j^1, \cdots, \theta_j^{q-1}, \theta_{j-1}^{q+1}, \cdots, \theta_{j-1}^{N_n}\right) \\ &\propto P\left(\mathbf{z}_1^q | \mathbf{x}_1^q\right) \int P\left(\mathbf{x}_1^q | \mathbf{x}_0^q\right) P\left(\mathbf{x}_0^q\right) d\mathbf{x}_0^q \\ &\times \left(\prod_{r=1}^{q-1} P\left(\mathbf{z}_1^{r \leftrightarrow q} | \mathbf{x}_1^r = \theta_j^r, \mathbf{x}_1^q\right)\right) \\ &\times \left(\prod_{r=q+1}^{N_n} P\left(\mathbf{z}_1^{r \leftrightarrow q} | \mathbf{x}_1^r = \theta_{j-1}^r, \mathbf{x}_1^q\right)\right) \end{aligned} \tag{5}$$

From the second time step onward, the nodes become cross-correlated. Hence, for each time step $k > 1$ and for each auxiliary node q at each scan $j \geq 1$, we sample:

$$\begin{aligned} \theta_j^q &\sim P\left(\theta^q | \theta_j^1, \cdots, \theta_j^{q-1}, \theta_{j-1}^{q+1}, \cdots, \theta_{j-1}^{N_n}\right) \\ &\propto P\left(\mathbf{x}_k^q | \mathbf{z}_k^q\right) \left(\prod_{r=1}^{q-1} P\left(\mathbf{z}_k^{r \leftrightarrow q} | \mathbf{x}_k^r = \theta_j^r, \mathbf{x}_k^q\right)\right) \\ &\times \left(\prod_{r=q+1}^{N_n} P\left(\mathbf{z}_k^{r \leftrightarrow q} | \mathbf{x}_k^r = \theta_{j-1}^r, \mathbf{x}_k^q\right)\right) \end{aligned} \tag{6}$$

Then for the primary node p at the scan, we sample:

$$\begin{aligned} \theta_j^p &\sim P\left(\theta^p | \theta_j^1, \cdots, \theta_j^{p-1}, \theta_j^{p+1}, \cdots, \theta_j^{N_n}\right) \\ &\propto P\left(\mathbf{z}_k^p | \mathbf{x}_k^p\right) \int P\left(\mathbf{x}_k^p | \mathbf{x}_{k-1}^p\right) P\left(\mathbf{x}_{k-1}^p | \mathbf{Z}_{1:k-1}\right) d\mathbf{x}_{k-1}^p \\ &\times \left(\prod_{r=1, r \neq p}^{N_n} P\left(\mathbf{z}_k^{r \leftrightarrow p} | \mathbf{x}_k^r = \theta_j^r, \mathbf{x}_k^p\right)\right) \end{aligned} \tag{7}$$

Iterative runs of Equations (6) and (7) generate a Gibbs chain at each time step. Figure 2 demonstrates one of the scans in the sampling process. Following a sufficient burn-in period (of, say, N_{bp} scans), the chain approaches its stationary distribution. From the Gibbs chain we then extract a set of particles to approximate the marginal posterior distribution of the primary node $P\left(\mathbf{x}_k^p | \mathbf{Z}_{1:k}\right)$. Theoretically, the desired posterior distribution could be approximated to any degree of accuracy with sufficient number of particles. To reduce autocorrelation, samples are extracted with a sampling interval of N_{si} (or a thinning ratio of $1/N_{si}$ in other words), i.e., by taking every $(N_{si})^{th}$ value in the chain. Please note that the extracted posterior particles have equal weights, therefore the resampling process is not required any more.

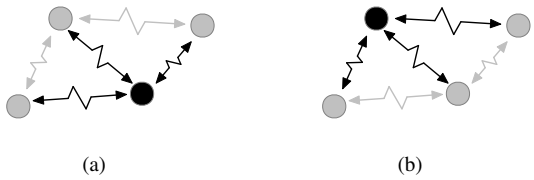

(a) (b)

Fig. 3. Primary and auxiliary nodes. An arbitrary node works as the primary node in a) while the rest are auxiliary nodes. In b) another node becomes the primary node. This goes on so that every node is treated as the primary node. The processing of these four primary nodes in the figure is independent from each other, therefore computation for them could be processed in parallel.

By repeating the above algorithm for every primary node at time k, all nodes are updated cooperatively with both egocentric and relative observations in $\mathbf{Z}_k$. Figure 3 illustrates how each node is treated as the primary node in parallel.

C. Optimisations

1) Construction of Uninformative Distribution for Auxiliary Nodes: In Equation (6), the prior distribution of an auxiliary node q at each iteration is constructed with $P\left(\mathbf{x}^q | \mathbf{z}_k^q\right)$ when it exists. In cases where the auxiliary node is out of egocentric observations, the $P\left(\mathbf{x}^q | \mathbf{z}_k^q\right)$ must be replaced by an uninformative distribution. Ideally, the uninformative distribution is a uniform distribution over the entire state space, which is not feasible to create. Instead, a regional uninformative distribution around the possible area of the auxiliary node's location is constructed. Given an arbitrary proposed distribution $q(\mathbf{x})$ that is easy to sample from (say, Gaussian distribution), a regional uniform distribution could be obtained by dividing the proposed distribution by itself. This means for particle $i = 1$ to L, we draw $\{\mathbf{x}^{(i)}, w^{(i)}\} \sim q(\mathbf{x})$, then $w^{(i)} = w^{(i)}/q(\mathbf{x}^{(i)})$. Lastly, the obtained set of weights are normalised. Figure 4 demonstrates such an example in 2D space, compared to its ideal distribution.

2) Pre-Processing of the Primary Node: In the naive implementation of the GSCPF, each extraction from the Gibbs chain produces only one posterior particle for the primary node. In order to collect in total L posterior particles, the chain should meet a length of exactly $N_{cl} = N_{si} \times L$ scans after the burning-period. An improvement to the GSCPF is to extract and accumulate the updated set of weights when it comes to each $(N_{si})^{th}$ scan in the chain. When all scans finish, the accumulated weights are normalised to yield the

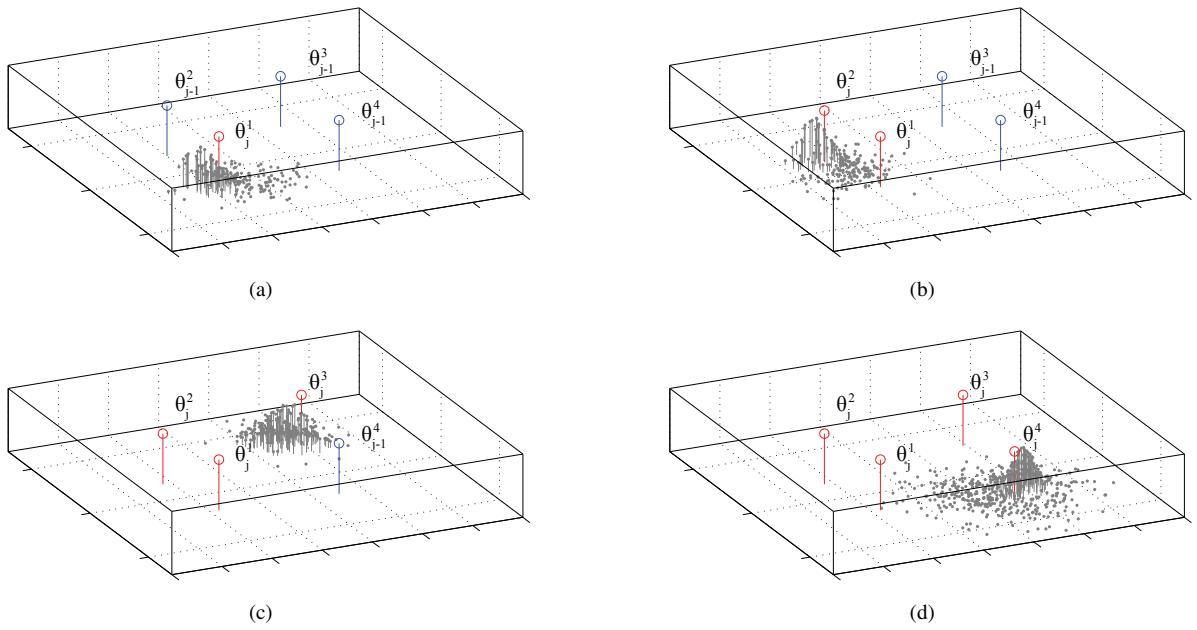

Fig. 2. A scan in the Gibbs sampling for four nodes. (a) to (c) show the sampling for three auxiliary nodes and at last (d) for the primary node.

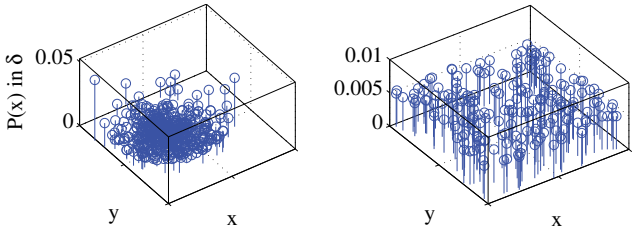

(a) Regional (b) Ideal

Fig. 4. Uninformative distributions in 2D space. The distribution in (a) uses $\mathcal{N}\left(\begin{bmatrix}40\\60\end{bmatrix}, \begin{bmatrix}15^2 & 0\\0 & 15^2\end{bmatrix}\right)$ as the proposed distribution.

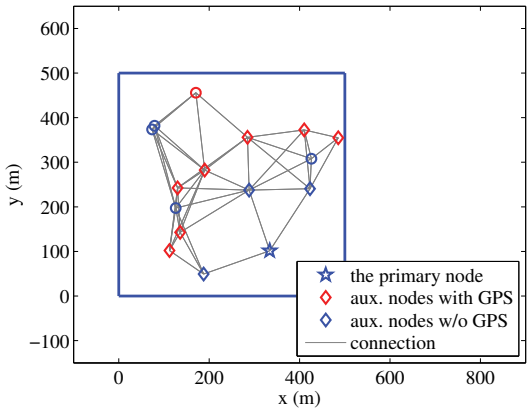

Fig. 5. An example of informative auxiliary nodes. The nodes with GPS enabled are in red, while those without GPS information are in blue.

set of posterior particles. The improvement brings a flexible requirement on the length of the Gibbs chain, and thus the computation cost could be reduced. Regardless of the chain length N_{cl}, the quantity of the posterior particles is kept identical to the prior. Nevertheless, the resampling process should be used when the quantity of effective particles $\widehat{N_{eff}}$ is below a threshold N_{thr}, to prevent particle degeneracy. The improved algorithm is shown in Table I in the form of pseudocode. Please note that the process of the first iteration is not included in the table.

3) Selection of Informative Auxiliary Nodes from Neighbours: The approach could be optimised in MANETs. As long as every node links into the network, a node i is an N-hop ($N \geq 1$) neighbour of another arbitrary node j. The gain from the information of the node i tends to be negligible when the N is large, as the information gets diluted along with transmission. For this reason, in order to reduce the problem complexity, only a fraction of all other nodes are used as the auxiliary nodes to the primary node. Specifically, the algorithm considers a node as an informative auxiliary when one of the following criteria is met:

- It is a 1-hop neighbour with GPS enabled, as it is informative to the primary node.
- It is considered an informative 1-hop neighbour without GPS information, when it connects to at least one node with GPS enabled and therefore could provide second-hand position information.
- It is a 2-hop neighbour with GPS enabled and connected by any of informative 1-hop neighbours, i.e., those falling in one of above two.

Note that the selection process of auxiliary nodes is performed for each primary node at every iteration, therefore, each will have its own dynamic list of auxiliary nodes according to the instantaneous network topology. At each iteration, the algorithm executes the Gibbs sampling for every primary node individually. See Figure 5 for an example of informative auxiliary nodes selected for a primary node.

D. Centralised and Decentralised Implementation

The algorithm can be implemented in a centralised or decentralised architecture. When the centralised structure is used, at every iteration, both absolute and relative observations are forwarded to the base station for updating the estimates via a communication network. If the tracking is realised in a decentralised manner, each node keeps sharing its egocentric observations and pairwise measurements with its instant neighbours. In the meanwhile, every node performs self-localisation using its own egocentric information and all available information it receives. In this case, only the node itself is treated as the primary node. The computation burden is hence distributed over all nodes in the field.

In both centralised and decentralised frameworks, what is transmitted between nodes is the observation data only. State estimates are not required to be transmitted.

V. Test with Non-Gaussian Cases

A. Setup

The proposed GSCPF was tested in cases with the presence of non-Gaussian noises in relative range observations. The purpose was to evaluate the performance of the algorithm when the Gaussian assumption is not valid, which is true for most real world applications. In the test, 16 mobile nodes moved within a square field with a dimension of $500m \times 500m$. Only half of the mobile nodes had absolute egocentric position information provided by on-board GPS sensors. The radio communication device mounted on each mobile node enabled it to communicate with others within a limited range, and to measure relative range between the nodes with some noise. A central station was adopted to collect real-time observations from each mobile node via multi-hop communication. It was at the central station where the global tracking took place.

Initially, 16 mobile nodes were positioned in the form of a 4×4 array with even intervals, as shown in Figure 6. Trajectories of the nodes in one of the testing cases are also shown in the figure. The EKF was used as a comparison to the proposed GSCPF algorithm. Both filters were tracking the state of each node, which is composed of positions and velocities in two dimensions.

$$\mathbf{x} = \begin{bmatrix} r_x & r_y & v_x & v_y \end{bmatrix}^T$$

In the EKF, the non-linear relative ranging model between two neighbouring nodes in 2D space was linearised. A Student's *t*-distribution was chosen and used in the test. The distribution is similar to Gaussian but comparatively heavier-tailed, which means that it is more likely to produce samples that fall far from its mean. In the limit $\nu \to \infty$, the Student's *t*-distribution turns into a Gaussian:

$$\lim_{\nu \to \infty} St\left(\mu, \lambda, \nu\right) = \mathcal{N}\left(\mu, \sigma^2\right)$$

where μ is mean; λ is precision; ν is degrees of freedom; and variance $\sigma^2 = \frac{1}{\lambda}\frac{\nu}{\nu-2}$ $(\nu > 2)$.

TABLE I
Algorithm: GSCPF

$\Theta_k \leftarrow$ *Partile_Filter* $\left(\Theta_{k-1}, \mathbf{Z}_k\right)$

par for $p = 1$ to N_n **do**
  load prior particles $\{\mathbf{x}_{k-1}^{p,(i)}, w_{k-1}^{p,(i)}\}_{i=1}^{L}$ from Θ_{k-1}
  Intra-node Fusion:
  predict $P\left(\mathbf{x}_k^p|\mathbf{Z}_{1:k-1}\right)$ from $P\left(\mathbf{x}_{k-1}^p|\mathbf{Z}_{1:k-1}\right)$
  update $P\left(\mathbf{x}_k^p|\mathbf{Z}_{1:k}\right)^- \propto P\left(\mathbf{z}_k^p|\mathbf{x}^p\right) P\left(\mathbf{x}_k^p|\mathbf{Z}_{1:k-1}\right)$
    $\{\mathbf{x}_k^{p,(i)}, w_{k-}^{(i)}\}_{i=1}^{L} \sim P\left(\mathbf{x}_k^p|\mathbf{Z}_{1:k}\right)^-$
  initialise weights $\{w_k^{p,(i)}\}_{i=1}^{L} = 0$
  initialise Gibbs variables $\theta^1 = \theta_0^1, \cdots, \theta^{N_n} = \theta_0^{N_n}$
  for $j = 1$ to $(N_{bp} + N_{cl})$ **do**
    Sampling for each auxiliary node:
    for $q = 1$ to $p-1$, $p+1$ to N_n **do**
      $\theta_j^q \sim P\left(\theta^q|\theta_j^1, \cdots, \theta_j^{q-1}, \theta_{j-1}^{q+1}, \cdots, \theta_{j-1}^{N_n}\right)$
      with observations from $\mathbf{Z}_k$ fused in
    end for
    Sampling for the primary node:
    Inter-node Fusion:
    likelihood $\Lambda = \prod_{r=1, r\neq p}^{N_n} P\left(\mathbf{z}_k^{r\leftrightarrow p}|\mathbf{x}^r = \theta_j^r, \mathbf{x}^p\right)$
    update $P\left(\mathbf{x}_k^p|\mathbf{Z}_{1:k}\right)^+ \propto \Lambda P\left(\mathbf{x}_k^p|\mathbf{Z}_{1:k}\right)^-$
      $\{\mathbf{x}_k^{p,(i)}, w_{k+}^{(i)}\}_{i=1}^{L} \sim P\left(\mathbf{x}_k^p|\mathbf{Z}_{1:k}\right)^+$
    draw $\theta_j^p \sim P\left(\mathbf{x}_k^p|\mathbf{Z}_{1:k}\right)^+$
    if $(j - N_{bp})$ is an integer times of N_{si} **do**
      Accumulate weights:
      $\{w_k^{p,(i)}\}_{i=1}^{L} = \{w_k^{p,(i)}\}_{i=1}^{L} + \{w_{k+}^{(i)}\}_{i=1}^{L}$
    end if
  end for
  normalise weights $\{w_k^{p,(i)}\}_{i=1}^{L}$
  if $\widehat{N_{eff}} < N_{thr}$ **do**
    resample with replacement L particles from $\{\mathbf{x}_k^{p,(i)}, w_k^{p,(i)}\}_{i=1}^{L}$ according to $\{w_k^{p,(i)}\}_{i=1}^{L}$
  end if
  save posterior particles $\{\mathbf{x}_k^{p,(i)}, w_k^{p,(i)}\}_{i=1}^{L}$ to Θ_k
end for

In the test, the GSCPF would use the exact Student's *t*-distribution parameters in Figure 7 to build up its observation model, while the EKF used the Gaussian in the figure to approximate the *t*-distribution. The approximation is somewhat overconfident by excluding probabilities on the tails of the *t*-distribution. The approximation could never be perfect by using only one Gaussian. The rest of components involved in the test were kept the same, in order to make sure that it is only the relative observation models that would account for differences in tracking results of the two approaches. Detailed parameters used in the test could be found in Table II. These parameters were determined in order to produce explicit results. The algorithm calculated one iteration per second of time. Some location errors were intentionally added to every node in the initial state.

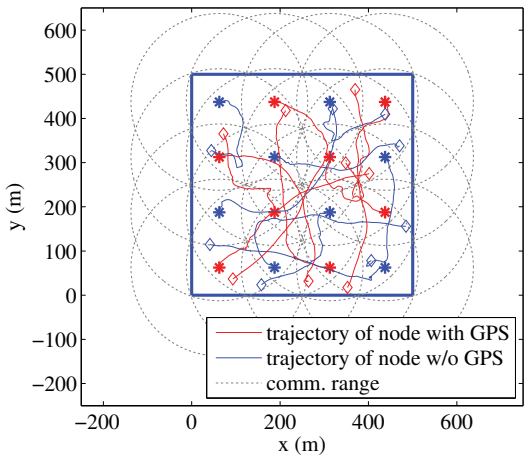

Fig. 6. Initial positions and true trajectories of mobile nodes. Each mobile node moves with random accelerations within the square field, with starting point represented by asterisk and ending point denoted by diamond shape. Each dashed circle represents the coverage of wireless communication of a node.

B. Performance Metrics

To quantify tracking accuracy, root mean square error (RMSE) was used as a measure. The RMSE of location of overall N_n mobile nodes in a 2D plane is computed by:

$$RMSE = \sqrt{\frac{\sum_{p=1}^{N_n} \left(\hat{r}_x^p - r_x^p\right)^2 + \left(\hat{r}_y^p - r_y^p\right)^2}{N_n}}$$

A similar equation is used to calculate the RMSE value in velocity. In addition, normalised estimation error squared (NEES) was adopted in the test as the metrics of consistency of the two tracking approaches. The NEES value for a given mobile node at time k is calculated by:

TABLE II
TESTING PARAMETERS

Parameter	Value
total Monte Carlo cases	30
total iterations per case	200
total nodes N_n	16
total nodes with GPS enabled	8
acceleration noise in x and y	$\mathcal{N}\left(\left[\begin{smallmatrix}0\\0\end{smallmatrix}\right], \left[\begin{smallmatrix}0.2^2 & 0\\0 & 0.2^2\end{smallmatrix}\right]\right)$
position obs. noise in x and y	$\mathcal{N}\left(\left[\begin{smallmatrix}0\\0\end{smallmatrix}\right], \left[\begin{smallmatrix}5^2 & 0\\0 & 5^2\end{smallmatrix}\right]\right)$
distance obs. noise in EKF	$\mathcal{N}\left(0, 10^2\right)$
distance obs. noise in GSCPF	$St\left(0, 0.03, 3\right)$
initial position interval	125 m
P2P communication range	200 m
particles for primary node N_p	2000
particles for auxiliary node N_a	1000
burn-in length N_{bp}	200
sampling interval N_{si}	5
length of Gibbs chain N_{cl}	2000

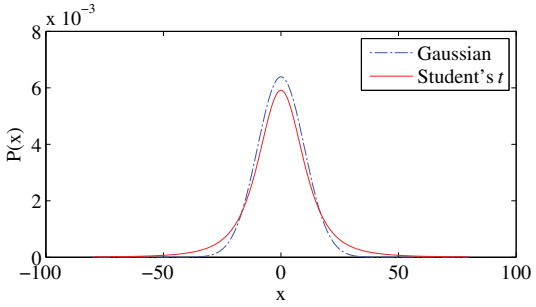

Fig. 7. Gaussian and non-Gaussian distributions. The blue curve demonstrates a zero-mean Gaussian distribution described by $\mathcal{N}\left(0, \sigma^2\right)$ where $\sigma = 10$. The red shows a Student's t-distribution as an example of non-Gaussian distributions. It is similar to the Gaussian but comparatively heavier-tailed. It is formulated by $St\left(0, \lambda, \nu\right)$ where $\nu = 3$ is degrees of freedom, and the precision $\lambda = \frac{1}{\sigma^2}\frac{\nu}{\nu-2} = 0.03$. Along with the growing of ν to ∞, the Student's t-distribution approaches the Gaussian one.

$$\epsilon\left(k\right) = \left(\hat{\mathbf{x}}_k - \mathbf{x}_k\right)^T \mathbf{P}_k^{-1} \left(\hat{\mathbf{x}}_k - \mathbf{x}_k\right)$$

where $\hat{\mathbf{x}}_k$ is the state estimate at time k, $\mathbf{x}_k$ is its true value, and $\mathbf{P}_k$ is its associated covariance at time k.

The consistency test was based on averaging NEES results over N Monte Carlo runs of a filter, which yields:

$$\bar{\epsilon}\left(k\right) = \frac{1}{N}\sum_{i=1}^{N} \epsilon^i\left(k\right)$$

Then the $N\bar{\epsilon}\left(k\right)$ will have a χ^2 (chi-square) distribution with $Ndim\left(\mathbf{x}_k\right)$ degrees of freedom [24] [7], under the hypothesis that the tested filter is consistent and approximately linear and Gaussian. The state estimation errors are considered consistent with the filter-calculated covariances if $\bar{\epsilon}\left(k\right) \in \left[r_1, r2\right]$, where the interval $\left[r_1, r2\right]$ bounds the two-sided 95% probability concentration region and is calculated by $\left[\chi^2_{Ndim(\mathbf{x}_k)}\left(0.025\right)/N, \chi^2_{Ndim(\mathbf{x}_k)}\left(0.975\right)/N\right]$.

A filter tends to produce optimistic estimates if the $\bar{\epsilon}\left(k\right)$ rises significantly higher than the upper bound, while if it stays below the lower bound for a majority of time, the filter is considered conservative [25].

C. Results

The GSCPF algorithm performed better than the EKF in both position and velocity estimation in the 2D MANET cases, according to the testing results illustrated in Figure 8. In all $N = 30$ Monte Carlo cases tested, the EKF performed the estimation given the full knowledge of observations generated about every mobile node. On the other hand, the GSCPF tracked these nodes only based on a subset of all available information, which was automatically picked based on the informative auxiliary nodes selection mechanism presented in Section IV-C.3. The mechanism aims to reduce computational burden by excluding those neighbours not considered sufficiently informative. This certainly results in a sacrifice in the tracking accuracy to some extent due to an information loss.

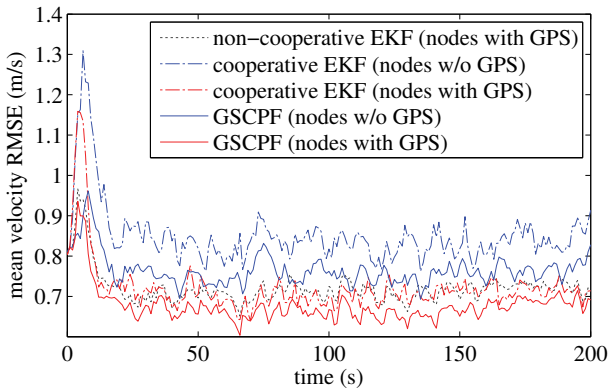

(a) Mean velocity RMSE

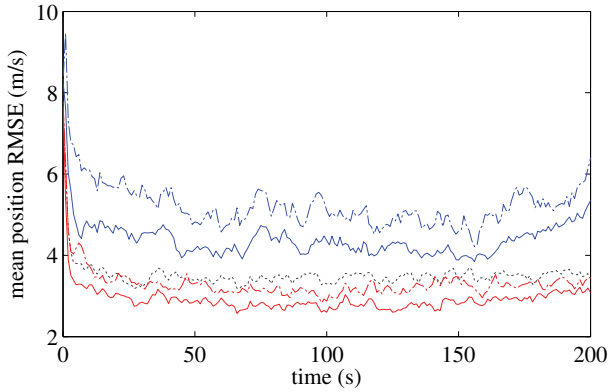

(b) Mean position RMSE

Fig. 8. Mean RMSEs of velocity and position. The mean RMSE results of GSCPF outperform EKF's in both (a) velocity and (b) position. The tracking results of independent EKF for nodes without GPS are not shown as the independent tracking algorithm fails in such scenarios.

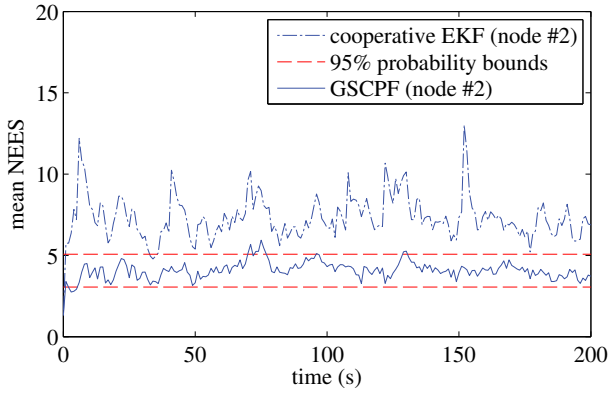

Fig. 9. NEES consistency test for the tracking of node #2. The in-bound rate of the GSCPF tracking result is about 93.03%, while most of the time the EKF result is out of the 95% probability bounds.

Nevertheless, it is observed in Figure 8 that generally the GSCPF tracked nodes more accurately than the EKF in the test. In these non-linear and non-Gaussian testing cases, errors were introduced into the EKF during the approximation of non-Gaussian noises and linearisation of the inter-node observation model. We believe that the errors accounted for an even larger degradation of performance in the EKF, compared to what the information loss did in the GSCPF.

Furthermore, the results of NEES shown in Figure 9 also suggest better estimation consistency of the GSCPF algorithm than that of the EKF, under the particular testing environment. The figure illustrates the result for one of the nodes, and a similar result is concluded about every other node. As previously mentioned, the Student's t-distribution is more likely to generate samples that are far away from its mean because of its "longer tails" than its Gaussian approximation. However, the EKF is sensitive to the presence of observations that are considered "outliers", i.e., those fall further than what its Gaussian observation model predicts, thereby an over-optimistic tracking result is observed for the EKF in Figure 9. This is not an issue to the GSCPF as it has the real distribution of noises in observations more precisely modelled. The t-distribution in the test was used only as an example out of various types of non-Gaussian noises, which exist ubiquitously in the real world. From this point of view, the GSCPF, as a nonparametric approach, tends to be more robust than its parametric counterpart in practical implementation.

D. Effects of Parameters in the Gibbs Sampler

There are three important parameters in the Gibbs sampler: the Gibbs chain length N_{cl}, the Gibbs sampling interval N_{si}, and the effective sample size N_{es}. The greater N_{cl}, the higher computational cost; the larger N_{si}, the lower autocorrelation. Their relationship could be revealed by the equation: $N_{es} = N_{cl}/N_{si}$. Figure 10 evaluates the effects of these parameters on the tracking accuracy. As seen in the figure, the average RMSE decreases along with the increase of N_{si} or N_{cl}, or the particle quantity L for primary nodes. It can be concluded from the figure that, a reasonable value of N_{si}, say, 5 or 10, is recommended for a trade-off between the tracking accuracy and the computational cost. Numbers in these figures were achieved by averaging tracking results of 7 nodes (4 with GPS information known and 3 unknown) from 50 Monte Carlo cases of fully connected networks.

VI. Conclusions and Future Work

This paper presented a nonparametric approach to track multiple mobile nodes in a cooperative manner. Relative range information, together with egocentric position information from the mobile nodes that are equipped with GPS sensors, is shared among nodes and forwarded to a base station via a mobile ad-hoc network. The results show that it is possible to obtain accurate and consistent estimates of multiple nodes using the proposed algorithm.

In a practical application, not all mobile nodes will have continual access to GPS position information. Even when the GPS provides position information, there can be significant errors due to signal interference, multipath, poor satellite configuration, etc. The results presented in the paper demonstrate that the algorithms can improve the position estimates of mobile nodes with and without egocentric position information available. Furthermore, the results demonstrate superior performance of the proposed approach to that of

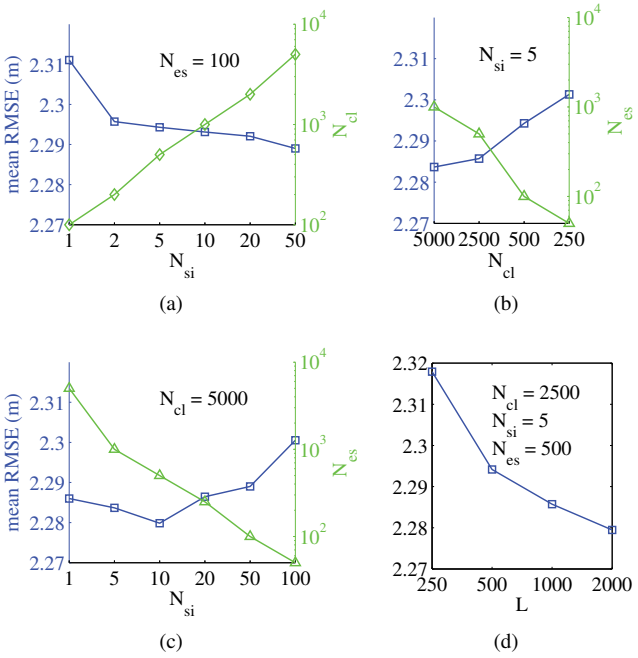

Fig. 10. Average position RMSEs with different parameters. (a) and (b) show the descent in average RMSE along with the ascents of N_{si} and N_{cl}, respectively. The x-axis in (b) is intentionally inverted in order to help understand (c). When the length of Gibbs chain N_{cl} is fixed, it is seen from (c) that the average RMSE reaches a trough at the point $N_{si} = 10$. This phenomenon could be explained by a combined effect of N_{si} and N_{es} shown in (a) and (b), respectively. Before the point, the result is dominated by the improvement of accuracy brought by a larger N_{si}. However after this point, the degradation in accuracy due to a smaller N_{es} becomes manifest and dominates the result. (d) illustrates the decrease of RMSE when a larger quantity of particles is adopted for primary nodes.

the EKF in applications with the presence of non-Gaussian properties. This approach is now being extended and applied to the tracking of a fleet of vehicles in a large mining environment, where inter-vehicle communication is intermittent. This involves delayed-state cooperative tracking with time delayed observations, highly non-linear and non-Gaussian properties in motion dynamics and position observations. Encouraging experiment results have been obtained.

The future work will include a more detailed investigation into the fundamental principle of the Gibbs sampler based tracking framework. Furthermore, the algorithm will be optimised toward a more efficient sampling process and a reduced computational cost.

REFERENCES

[1] H. Wymeersch, J. Lien, and M. Z. Win, "Cooperative localization in wireless networks," *Proc. of the IEEE*, vol. 97, no. 2, pp. 427–450, Feb. 2009.

[2] T. Eren, "Cooperative localisation in wireless ad hoc and sensor networks using hybrid distance and bearing (angle of arrival) measurements," *EURASIP Journal on Wireless Communications and Networking*, pp. 541–552, Aug. 2011, 2011:72.

[3] W. Chen and X. Meng, "A cooperative localization scheme for zigbee-based wireless sensor networks," in *Proc. the 14th IEEE International Conference (ICON'06)*, vol. 2, Sep. 2006, pp. 1–5.

[4] L.-L. Ong, T. Bailey, and H. Durrant-Whyte, "Decentralised particle filtering for multiple target tracking in wireless sensor networks," in *Proc. the 11th International Conference on Information Fusion*, United States, Jun. 2008, pp. 342–349.

[5] L. Dong, "Cooperative localisation and tracking of mobile ad hoc networks," *IEEE Trans. Signal Processing*, vol. 60, no. 7, pp. 3907–3913, Jul. 2012.

[6] Y. P. Fallah, C.-L. Huang, R. Sengupta, and H. Krishnan, "Analysis of information dissemination in vehicular ad-hoc networks with application to cooperative vehicle safety systems," *IEEE Trans. Veh. Technol.*, vol. 60, no. 1, pp. 233–247, Jan. 2011.

[7] A. Bahr, M. R. Walter, and J. J. Leonard, "Consistent cooperative localisation," in *Proc. IEEE International Conference on Robotics and Automation (ICRA'09)*, Kobe, Japan, May 2009.

[8] G. P. Huang, N. Trawny, A. I. Mourikis, and S. I. Roumeliotis, "Observability-based consistent EKF estimators for multi-robot cooperative localization," *Auton. Robots*, vol. 30, no. 1, pp. 99–122, 2011.

[9] K. Y. K. Leung, T. D. Barfoot, and H. H. T. Liu, "Decentralised localisation of sparsely-communicating robot networks: A centralised-equivalent approach," *IEEE Trans. Robot.*, vol. 26, no. 1, pp. 62–77, Feb. 2010.

[10] N. Patwari, A. O. Hero-III, M. Perkins, N. S. Correal, and R. J. O'Dea, "Relative location estimation in wireless sensor networks," *IEEE Trans. Signal Processing*, vol. 51, no. 8, pp. 2137–2148, Aug. 2003.

[11] E. D. Nerurkar, S. I. Roumeliotis, and A. Martinelli, "Distributed maximum a posteriori estimation for multi-robot cooperative localisation," in *Proc. IEEE International Conference on Robotics and Automation (ICRA'09)*, Kobe, Japan, May 2009.

[12] B. H. Cheng, R. E. Hudson, F. Lorenzelli, L. Vandenberghe, and K. Yao, "Distributed Gauss-Newton method for node localisation in wireless sensor networks," in *Proc. of the 6th IEEE Workshop on Signal Processing Advances in Wireless Communications (SPAWC2005)*, New York, USA, Jun. 2005.

[13] N. A. A. K. Pahlavan, B. Alavi, and X. Li, "A novel cooperative localisation algorithm for indoor sensor networks," in *Proc. the 17th Annual IEEE International Symposium on Personal, Indoor and Mobile Radio Communications (PIMRC'06)*, Helsinki, Finland, Sep. 2006.

[14] T. Sathyan and M. Hedley, "A particle filtering algorithm for cooperative tracking of nodes in wireless networks," in *Proc. the 22nd IEEE International Symposium on Personal, Indoor and Mobile Radio Communications (PIMRC'11)*, 2011, pp. 1304–1308.

[15] A. Howard, M. J. Matarić, and G. S. Sukhatme, "Putting the 'I' in 'team': an ego-centric approach to cooperative localisation," in *Proc. IEEE International Conference on Robotics and Automation (ICRA'03)*, Taipei, Taiwan, Sep. 2003.

[16] D. Fox, W. Burgard, H. Kruppa, and S. Thrun, "A probabilistic approach to collaborative multi-robot localisation," *Auton. Robots*, vol. 8, no. 3, pp. 325–344, Jun. 2000.

[17] C. Snyder, T. Bengtsson, P. Bickel, and J. Anderson, "Obstacles to high-dimensional particle filtering," *Monthly Weather Review*, vol. 136, no. 12, pp. 4629–4640, 2008.

[18] A. Doucet, N. de Freitas, K. Murphy, and S. Russell, "Rao-Blackwellised particle filtering for dynamic Bayesian networks," in *Proc. the 16th Annual Conference on Uncertainty in Artificial Intelligence (UAI'00)*, San Francisco, California, USA, 2000, pp. 176–183.

[19] A. T. Ihler, J. W. Fisher, R. L. Moses, and A. S. Willsky, "Nonparametric belief propagation for self-localisation of sensor networks," *IEEE Journal on Selected Areas in Communications*, vol. 23, no. 4, pp. 809–819, 2005.

[20] V. Savic and S. Zazo, "Cooperative localisation in mobile networks using nonparametric variants of belief propagation," *Ad Hoc Networks*, vol. 11, pp. 138–150, 2013.

[21] Y. Weiss, "Correctness of local probability propagation in graphical models with loops," *Neural Computation*, vol. 12, no. 1, pp. 1–41, 2000.

[22] J. S. Yedidia, W. T. Freeman, and Y. Weiss, "Constructing free energy approximations and generalised belief propagation algorithms," *IEEE Trans. Inform. Theory*, vol. 51, pp. 2282–2312, 2005.

[23] V. Savic, A. Población, S. Zazo, and M. García, "Indoor positioning using nonparametric belief propagation based on spanning trees," *EURASIP Journal on Wireless Communications and Networking*, vol. 2010, 2010.

[24] Y. Bar-Shalom, X.-R. Li, and T. Kirubarajan, *Estimation with Applications to Tracking and Navigation*. John Wiley and Sons, 2001.

[25] T. Bailey, J. Nieto, J. Guivant, M. Stevens, and E. Nebot, "Consistency of the EKF-SLAM algorithm," in *Proc. IEEE/RSJ International Conference of Intelligent Robots and Systems (IROS)*, Beijing, China, Oct. 2006.